

CSUHEP 02-01  
 DAPNIA-02-95  
 LAL-02-83

# Measuring the Weak Phase $\gamma$ in Color Allowed $B \rightarrow DK\pi$ Decays

Roy Aleksan

*Centre d'Etudes Nucleaires, Saclay, DAPNIA/SPP, F-91191 Gif-sur-Yvette, CEDEX,  
 France*

Troels C. Petersen

*LAL Bat 208, Orsay BP 34, 91898 France*

Abner Soffer

*Department of Physics, Colorado State University, Fort Collins, CO 80523, U.S.A.  
 (October 25, 2018)*

## Abstract

We present a method to measure the weak phase  $\gamma$  in the three-body decay of charged  $B^\pm$  mesons to the final states  $DK^\pm\pi^0$ . These decays are mediated by interfering amplitudes which are color-allowed and hence relatively large. As a result, large CP violation effects that could be observed with high statistical significance are possible. In addition, the three-body decay helps resolve discrete ambiguities that are usually present in measurements of the weak phase. The experimental implications of conducting these measurements with three-body decays are discussed, and the sensitivity of the method is evaluated using a simulation.

## I. INTRODUCTION

CP violation is currently the focus of a great deal of attention. Since the start of operation of the B-factories, the standard model description of CP violation via the Cabibbo-Kobayashi-Maskawa (CKM) matrix [1] is being tested with increasing precision. BaBar [2] and Belle [3] have recently published measurements of the CKM parameter  $\sin(2\beta)$ , where  $\beta = \arg(-V_{cd}V_{cb}^*/V_{td}V_{tb}^*)$ , verifying the CKM mechanism to within the experimental sensitivity. Although improved measurements of  $\sin(2\beta)$  and  $B_s - \overline{B}_s$  mixing will probe the theory with greater scrutiny during the next few years, the measurement of the other angles of the unitarity triangle are necessary for a comprehensive study of CP violation.

Important constraints on the theory will be obtained from measurements of the CKM phase  $\gamma = \arg(-V_{ud}V_{ub}^*/V_{cd}V_{cb}^*)$ . A promising method for measuring this phase in the  $B$  system has been proposed [4]. Although this method involves color-allowed decays and hence offers favorable rates, it makes use of  $B_s$  mesons, which are not produced at B-Factories operating at the  $\Upsilon(4S)$  resonance. By contrast, the extraction of  $\gamma$  using the  $B_u$  and  $B_d$  system generally involves decays which are highly suppressed or difficult to reconstruct. In addition, these methods are generally subject to an eight-fold ambiguity due to *a-priori* unknown strong phases [4,5]. As a result, obtaining satisfactory sensitivity requires very high statistics and necessitates the use of as many decay modes and measurement methods as possible.

One important class of theoretically clean measurements will make use of decays of the type  $B \rightarrow DK$ . Gronau and Wyler [6] have proposed to measure  $\sin^2 \gamma$  in the interference between the  $\bar{b} \rightarrow \bar{c}u\bar{s}$  decay  $B^+ \rightarrow \overline{D^0}K^+$  and the color-suppressed  $\bar{b} \rightarrow \bar{u}c\bar{s}$  decay  $B^+ \rightarrow D^0K^+$ . Interference between these amplitudes takes place when the  $D$  meson is observed as one of the CP-eigenstates

$$D_{1,2} \equiv \frac{1}{\sqrt{2}} (D^0 \pm \overline{D^0}), \quad (1)$$

which are identified by their decay products, such as  $K^+K^-$  or  $K_s\pi^0$ . Several variations of this method have been developed [7–10], including addressing the effects of doubly Cabibbo-suppressed decays of the  $D$  meson [11] and mixing and CP-violation in the neutral  $D$  meson system [12], as well as insights to be gained from charm factory measurements [13].

A serious difficulty with measuring  $\gamma$  using  $B \rightarrow DK$  is that the  $\bar{b} \rightarrow \bar{u}c\bar{s}$  amplitude is expected to be extremely small. To a large degree, this is due to the color-suppression associated with the internal spectator diagram through which this amplitude proceeds. In the factorization model, color-suppression of the amplitude is parameterized by the phenomenological ratio  $|a_2/a_1|$ . This ratio is measured to be about 0.25 [14] by comparing decay modes which depend only on color-allowed amplitudes with those that depend on both color-allowed and color-suppressed amplitudes. With this value of  $|a_2/a_1|$ , one expects the amplitude ratio  $|\mathcal{A}(B^+ \rightarrow D^0K^+)/\mathcal{A}(B^+ \rightarrow \overline{D^0}K^+)|$  to be only about 0.1. The small branching fraction  $\mathcal{B}(B^+ \rightarrow D^0K^+)$  is therefore very difficult to measure with adequate precision, resulting in a large statistical error in the measurement of  $\sin^2 \gamma$ . The recent observation of the color-suppressed decays  $B^0 \rightarrow \overline{D^{(*)0}}\pi^0$ ,  $\overline{D^0}\eta$ , and  $\overline{D^0}\omega$  by Belle [15] and CLEO [16] has raised the possibility that  $|a_2/a_1|$  may be effectively larger in some modes. However, significant suppression is still expected for internal spectator diagrams.

This difficulty has led to attempts to address the problems presented by color suppression. Dunietz [7] proposed to apply the method to the decays  $B^0 \rightarrow DK^{*0}$ , making use of the fact that the decay  $K^{*0} \rightarrow K^+\pi^-$  tags the flavor of the  $B^0$ . In this mode, both the  $\bar{b} \rightarrow \bar{c}u\bar{s}$  and the  $\bar{b} \rightarrow \bar{u}c\bar{s}$  amplitudes are color suppressed, and hence of similar magnitudes, albeit small. Jang and Ko [9] and Gronau and Rosner [10] have devised a method in which the small branching fraction of the color-suppressed decay  $B^+ \rightarrow D^0K^+$  does not have to be measured directly. Rather, it is essentially inferred by using the larger branching fractions of the decays  $B^0 \rightarrow D^-K^+$ ,  $B^0 \rightarrow \bar{D}^0K^0$  and  $B^0 \rightarrow D_{1,2}K^0$ . Quantitative study suggests that the various alternative methods are roughly as sensitive as the method of Ref. [6], and are thus useful for increasing statistics and providing consistency checks [5].

## II. MEASURING $\gamma$ WITH COLOR-ALLOWED $B \rightarrow DK\pi$ DECAYS

In this paper we investigate a way to circumvent the color suppression penalty by using  $B^\pm$  decay modes which could potentially offer significantly large branching fractions, as well as large CP asymmetries. Similar modes involving neutral  $B$  decays can also be used. For example the final state  $D^0(\bar{D}^0)K^\pm\pi^\mp$  can be analyzed with the same technique as described here. Some other decays (such as  $B^0 \rightarrow D^-K_s\pi^+$ ) need a different treatment and will be discussed elsewhere [17]. The particular decays which are considered here are of the type  $B \rightarrow D^{(*)}K^{(*)}\pi(\rho)$ . These three body final states may be obtained by popping a  $q\bar{q}$  pair in color allowed decays. Although modes where one or more of the three final state particles is a vector can also be used, for clarity and simplicity only the mode  $B^\pm \rightarrow D^0K^\pm\pi^0$  is discussed here.

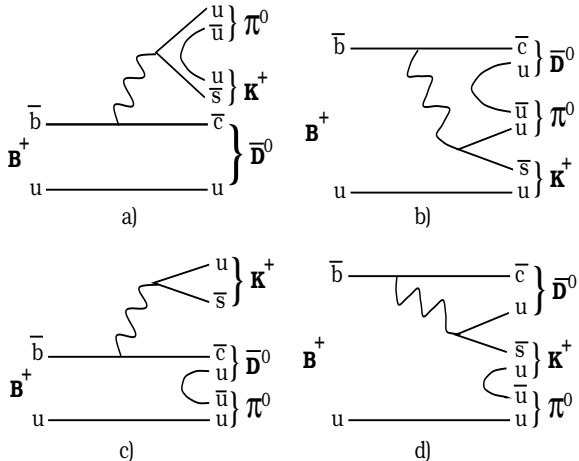


FIG. 1. Feynmann Diagrams for the decay  $B^+ \rightarrow \bar{D}^0K^+\pi^0$  involving the CKM matrix element product  $V_{cb}^*V_{us}$

Figs. 1 and 2 show the diagrams leading to the final states of interest. As can be seen, the leading diagrams (Fig. 1a and 2a) are both color-allowed and of order  $\lambda^3 = \sin(\theta_c)$  in the Wolfenstein parameterization [18], where  $\theta_c$  is the Cabibbo mixing angle. Due to the absence of color suppression, both interfering amplitudes are large, avoiding the complications which

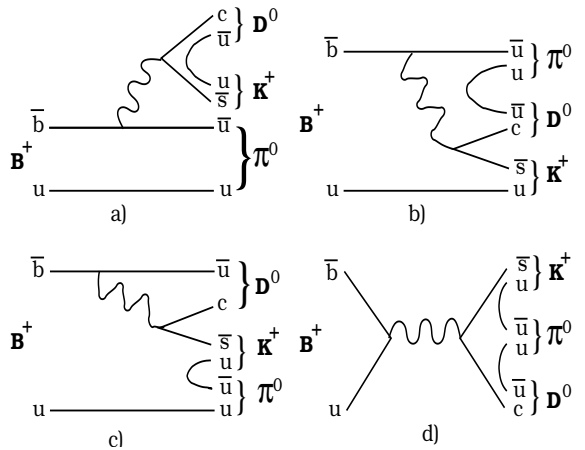


FIG. 2. Feynmann Diagrams for the decay  $B^+ \rightarrow D^0K^+\pi^0$  involving the CKM matrix element product  $V_{ub}^*V_{cs}$

arise due to the small magnitude of the  $\bar{b} \rightarrow \bar{u}c\bar{s}$  amplitude in the two-body decays. As a result, observable CP-violating effects in the three-body decays are expected to be large, and the  $\bar{b} \rightarrow \bar{u}c\bar{s}$  amplitude is more easily measured from the relatively large branching fraction  $\mathcal{B}(B^+ \rightarrow D^0 K^+ \pi^0)$ , which is now subject to significantly less contamination from doubly Cabibbo-suppressed  $D$  meson decays than the corresponding two-body modes. However, should the  $\bar{b} \rightarrow \bar{u}c\bar{s}$  amplitude be unexpectedly small, one could still carry out the analysis described in this paper by taking doubly Cabibbo-suppressed decays into account [5,11].

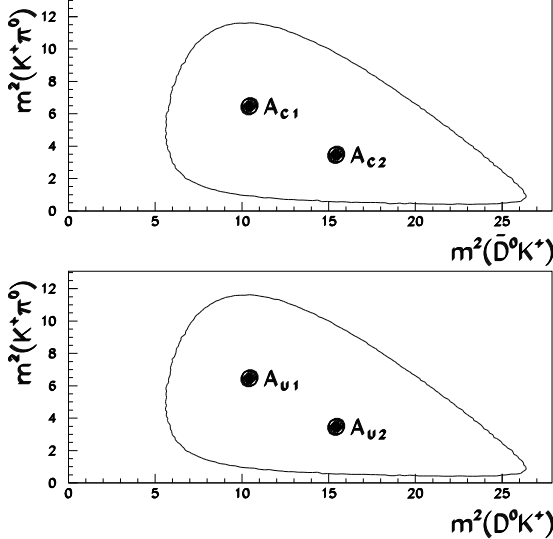


FIG. 3. Two points on the Dalitz plot of the decays  $B^+ \rightarrow \bar{D}^0 K^+ \pi^0$  and  $B^+ \rightarrow D^0 K^+ \pi^0$ .

Let us examine how one could observe CP violation and measure the angle  $\gamma$  in these decays. We first consider the case of very large statistics, and then discuss how one would proceed when the data sample is limited. Since we are dealing with a three-body decay, we use the Dalitz plot of the system  $DK^\pm\pi^0$  (see Fig. 3). Selecting a particular point  $i$  in this representation, Eq. (1) implies the relations

$$\begin{aligned} \mathcal{A}_i(B^+ \rightarrow D_{1,2}^0 K^+ \pi^0) &= \frac{1}{\sqrt{2}} (\mathcal{A}_i(B^+ \rightarrow D^0 K^+ \pi^0) \pm \mathcal{A}_i(B^+ \rightarrow \bar{D}^0 K^+ \pi^0)) \\ \mathcal{A}_i(B^- \rightarrow D_{1,2}^0 K^- \pi^0) &= \frac{1}{\sqrt{2}} (\mathcal{A}_i(B^- \rightarrow D^0 K^- \pi^0) \pm \mathcal{A}_i(B^- \rightarrow \bar{D}^0 K^- \pi^0)). \end{aligned} \quad (2)$$

Let us write the amplitudes corresponding to the transitions in Fig. 1 and 2 as

$$\begin{aligned} \mathcal{A}_i(B^+ \rightarrow \bar{D}^0 K^+ \pi^0) &= A_{ci} e^{i\delta_{ci}} \quad , \quad \mathcal{A}_i(B^+ \rightarrow D^0 K^+ \pi^0) = A_{ui} e^{i\delta_{ui}} e^{i\gamma}, \\ \mathcal{A}_i(B^- \rightarrow D^0 K^- \pi^0) &= A_{ci} e^{i\delta_{ci}} \quad , \quad \mathcal{A}_i(B^- \rightarrow \bar{D}^0 K^- \pi^0) = A_{ui} e^{i\delta_{ui}} e^{-i\gamma}, \end{aligned} \quad (3)$$

where  $\gamma$  is the relative phase of the CKM matrix elements involved in this decay, and  $A_c$  ( $A_u$ ) and  $\delta_c$  ( $\delta_u$ ) are the real amplitude and CP-conserving strong interaction phase of

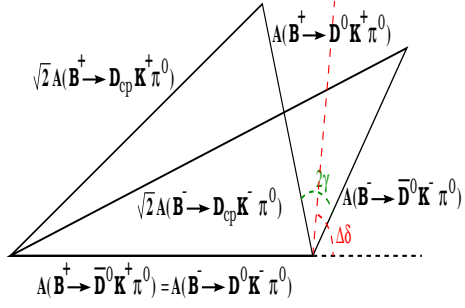


FIG. 4. Illustration of the triangle relations in the decays  $B^\pm \rightarrow \bar{D}^0 K^\pm \pi^0$  and  $B^\pm \rightarrow D^0 K^\pm \pi^0$ .

the transitions of Fig. 1 (Fig. 2). Let us note here that we have used the Wolfenstein parameterization at order  $\mathcal{O}(\lambda^3)$ . Should one use the full expansion, a small weak phase of order  $\lambda^4$  would be present. Indeed the angle which is measured is  $\gamma' = \arg(V_{ud}V_{ub}^*/V_{cs}V_{cb}^*) = \gamma + \xi$ , where  $\xi = \arg(-V_{cd}V_{cs}^*/V_{ud}V_{us}^*)$ . The angle  $\xi$  is one of the angles [19] arising from the unitarity relation  $V_{ud}V_{us}^* + V_{cd}V_{cs}^* + V_{td}V_{ts}^* = 0$ . The amplitudes in Eqs. 3 can be obtained from the measurements of the B decay widths

$$\begin{aligned}\Gamma_i(B^+ \rightarrow \overline{D^0}K^+\pi^0) &= \Gamma_i(B^- \rightarrow D^0K^-\pi^0) = A_{\mathcal{C}_i}^2 \\ \Gamma_i(B^+ \rightarrow D^0K^+\pi^0) &= \Gamma_i(B^- \rightarrow \overline{D^0}K^-\pi^0) = A_{\mathcal{U}_i}^2.\end{aligned}\quad (4)$$

Eq. (2) implies

$$\begin{aligned}2\Gamma_i(B^+ \rightarrow D_{1,2}^0K^+\pi^0) &= A_{\mathcal{C}_i}^2 + A_{\mathcal{U}_i}^2 \pm 2A_{\mathcal{C}_i}A_{\mathcal{U}_i}\cos(\Delta\delta_i + \gamma) \\ 2\Gamma_i(B^- \rightarrow D_{1,2}^0K^-\pi^0) &= A_{\mathcal{C}_i}^2 + A_{\mathcal{U}_i}^2 \pm 2A_{\mathcal{C}_i}A_{\mathcal{U}_i}\cos(\Delta\delta_i - \gamma),\end{aligned}\quad (5)$$

where  $\Delta\delta_i \equiv \delta_{\mathcal{U}_i} - \delta_{\mathcal{C}_i}$ . Thus, by measuring the widths in Eq. 4 and 5, one extracts  $\sin^2\gamma$  from

$$\sin^2\gamma = \frac{1}{2} \left( 1 - C\overline{C} \pm \sqrt{(1 - C^2)(1 - \overline{C}^2)} \right), \quad (6)$$

where  $C \equiv \cos(\Delta\delta_i + \gamma)$  and  $\overline{C} \equiv \cos(\Delta\delta_i - \gamma)$ . Hence in the limit of very high statistics, one would extract  $\sin^2\gamma$  for each point  $i$  of the Dalitz plot and therefore obtain many measurements of the same quantity. This would allow one to obtain a large set of redundant measurements from which a precise and consistent value of  $\sin^2\gamma$  could be extracted. We note that in our treatment we disregard doubly Cabibbo-suppressed  $D^0$  decays [11] since, due to the lack of color-suppression, their effect is small, and can be dealt with [5] in any case.

In every point of the Dalitz plot,  $\gamma$  is obtained with an eight-fold ambiguity, which is a consequence of the invariance of the  $\cos(\Delta\delta_i \pm \gamma)$  terms in Eq. (5) under the three symmetry operations [5]

$$\begin{aligned}S_{\text{ex}} &: \gamma \rightarrow \delta \quad , \quad \delta \rightarrow \gamma \\ S_{\text{sign}} &: \gamma \rightarrow -\gamma \quad , \quad \delta \rightarrow -\delta \\ S_\pi &: \gamma \rightarrow \gamma + \pi \quad , \quad \delta \rightarrow \delta + \pi.\end{aligned}\quad (7)$$

However, an important benefit is gained from the multiple measurements made in different points of the Dalitz plot. When results from the different points are combined, some of the ambiguity will be resolved, in the likely case that the strong phase  $\Delta\delta_i$  varies from one region of the Dalitz to the other. This variation can either be due to the presence of resonances or because of a varying phase in the non-resonant contribution. In this case, the exchange symmetry  $S_{\text{ex}}$  is numerically different from one point to the other, which in effect breaks this symmetry and resolves the ambiguity.

Similarly, the  $S_{\text{sign}}$  symmetry is broken if there exists some *a-priori* knowledge of the dependence of  $\Delta\delta_i$  on the Dalitz plot parameters. This knowledge is provided by the existence of broad resonances, whose Breit-Wigner phase variation is known and may be assumed to dominate the phase variation over the width of the resonance. To illustrate this, let  $i$  and  $j$

be two points in the Dalitz plot, corresponding to different values of the invariant mass of the decay products of a particular resonance. For simplicity we consider only one resonance. One then measures  $\cos(\Delta\delta_i \pm \gamma)$  at point  $i$  and  $\cos(\Delta\delta_i + \alpha_{ij} \pm \gamma)$  at point  $j$ , where  $\alpha_{ij}$  is known from the parameters of the resonance. It is important to note that the sign of  $\alpha_{ij}$  is also known, hence it does not change under  $S_{\text{sign}}$ . Therefore, should one choose the  $S_{\text{sign}}$ -related solution  $\cos(-\Delta\delta_i \mp \gamma)$  at point  $i$ , one would get  $\cos(-\Delta\delta_i + \alpha_{ij} \mp \gamma)$  at point  $j$ . Since this is different from  $\cos(\Delta\delta_i + \alpha_{ij} \pm \gamma)$ , the  $S_{\text{sign}}$  ambiguity is resolved. This is illustrated graphically in Eq. 8:

$$\begin{array}{ccc}
 \cos(\Delta\delta_i \pm \gamma) & \xrightarrow{S_{\text{sign}}} & \cos(-\Delta\delta_i \mp \gamma) \\
 BW \downarrow & & \downarrow BW \\
 \cos(\Delta\delta_i + \alpha_{ij} \pm \gamma) & \not\leftrightarrow & \cos(-\Delta\delta_i + \alpha_{ij} \mp \gamma)
 \end{array} \tag{8}$$

Thus, broad resonances reduce the initial eight-fold ambiguity to the two-fold ambiguity of the  $S_\pi$  symmetry, which is not broken. Fortunately,  $S_\pi$  leads to the well-separated solutions  $\gamma$  and  $\gamma + \pi$ , the correct one of which is easily identified when this measurement is combined with other measurements of the unitarity triangle.

### III. THE FINITE STATISTICS CASE

Since experimental data sets will be finite, extracting  $\gamma$  will require making use of a limited set of parameters to describe the variation of amplitudes and strong phases over the Dalitz plot. The consistency of this approach can be verified by comparing the results obtained from fits of the data in a few different regions of the Dalitz plot, and the systematic error due to the choice of the parameterization of the data may be obtained by using different parameterizations.

A fairly general parameterization assumes the existence of  $N_R$  Breit-Wigner resonances, as well as a non-resonant contribution:

$$\begin{aligned}
 \mathcal{A}_\xi(B^+ \rightarrow \overline{D^0} K^+ \pi^0) &= \left( A_{C0} e^{i\delta_{C0}} + \sum_{j=1}^{N_R} A_{Cj} B_{s_j}(\xi) e^{i\delta_{Cj}} \right) e^{i\delta_C(\xi)} \\
 \mathcal{A}_\xi(B^+ \rightarrow D^0 K^+ \pi^0) &= \left( A_{U0} e^{i\delta_{U0}} + \sum_{j=1}^{N_R} A_{Uj} B_{s_j}(\xi) e^{i\delta_{Uj}} \right) e^{i\delta_U(\xi)} e^{i\gamma},
 \end{aligned} \tag{9}$$

where  $\xi$  represents the Dalitz plot variables,

$$B_{s_j}(\xi) \equiv b_{s_j}(\xi) e^{i\delta_j(\xi)} \tag{10}$$

is the Breit-Wigner amplitude for a particle of spin  $s_j$ , normalized such that  $\int (b_{s_j}(\xi))^2 d\xi = 1$ ,  $A_{U0}$  and  $\delta_{U0}$  ( $A_{C0}$  and  $\delta_{C0}$ ) are the magnitude and CP-conserving phase of the non-resonant  $\bar{b} \rightarrow \bar{u}c\bar{s}$  ( $\bar{b} \rightarrow \bar{c}u\bar{s}$ ) amplitude, and  $A_{Uj}$  and  $\delta_{Uj}$  ( $A_{Cj}$  and  $\delta_{Cj}$ ) are the magnitudes and CP-conserving phase of the  $\bar{b} \rightarrow \bar{u}c\bar{s}$  ( $\bar{b} \rightarrow \bar{c}u\bar{s}$ ) amplitude associated with resonance  $j$  [20]. The functions  $\delta_C(\xi)$  and  $\delta_U(\xi)$  may be assumed to vary slowly over the Dalitz plot, allowing their description in terms of a small number of parameters. Eq. (1) again implies

$$\mathcal{A}_\xi(B^+ \rightarrow D_{1,2}^0 K^+ \pi^0) = \frac{1}{\sqrt{2}} \left( \mathcal{A}_\xi(B^+ \rightarrow D^0 K^+ \pi^0) \pm \mathcal{A}_\xi(B^+ \rightarrow \overline{D^0} K^+ \pi^0) \right). \quad (11)$$

The decay amplitudes of  $B^-$  mesons are identical to those of Eqs. (9) and (11), with  $\gamma$  replaced by  $-\gamma$ .

The decay amplitudes of Eqs. (9) and (11) can be used to conduct the full data analysis. This is done by constructing the probability density function (PDF)

$$P(\xi) = |\mathcal{A}_\xi(f)|^2, \quad (12)$$

where the amplitude  $\mathcal{A}_\xi(f)$  is given by one of the expressions of Eq. (9), Eq. (11), or their CP-conjugates, depending on the final state  $f$ . Given a sample of  $N_e$  signal events,  $\gamma$  and the other unknown parameters of Eq. (9) are determined by minimizing the negative log likelihood function

$$\chi^2 \equiv -2 \sum_{i=1}^{N_e} \log P(\xi_i), \quad (13)$$

where  $\xi_i$  are the Dalitz plot variables of event  $i$ .

#### IV. RESONANCES AND AMBIGUITIES

It is worthwhile to consider the resonances which may contribute to the  $D^0 K^\pm \pi^0$  final state. Obvious candidates are broad  $D^{**}$  and  $D_s^{**}$  states. However, only the ones which can decay as  $D^{**0} \rightarrow D^0 \pi^0$  or  $D_s^{**+} \rightarrow D^0 K^+$  are relevant for the final state of interest. This exclude the  $1^+$  states, which would decay to  $D^* \pi$  or  $D^* K$ . Furthermore, since the  $D_s^{**+}$  is essentially produced through a  $W^+$ , the  $2^+$  state is forbidden as well. Thus, one does not expect a large contribution from these states. A promising candidate might be the broad  $D_0^{*0}$  recently observed by the Belle collaboration [21]. We note that including such resonances in the analysis does not raise particular difficulties and would further enhance the sensitivity of the  $\gamma$  measurement. Similar arguments can be made for higher excited  $K$  states.

One also expects narrow resonances, such as the  $D^*(2007)^0$  and a narrow  $D_s^{**+}$  state, to be produced. However, as seen in the Dalitz plot of Fig. 5, these resonances do not overlap, and hence do not interfere. In addition, interference between a very narrow resonance and either a broad resonance or a non-resonant term is suppressed in proportion to the square root of the narrow resonance width. Therefore, narrow resonances contribute significantly to the CP violation measurement only if both the  $\bar{b} \rightarrow \bar{c}u\bar{s}$  and  $\bar{b} \rightarrow \bar{u}c\bar{s}$  amplitudes proceed through the same resonance. This scenario is favorable, but is not necessary for the success of our method, and will therefore not be focused on in the rest of this study.

In what follows, we discuss important properties of the method by considering the illustrative case, in which the  $\bar{b} \rightarrow \bar{u}c\bar{s}$  decay proceeds only via a non-resonant amplitude, and the  $\bar{b} \rightarrow \bar{c}u\bar{s}$  decay has a non-resonant contribution and a single resonant amplitude. For concreteness, the resonance is taken to be the  $K^{*\pm}(892)$ . We take the  $\xi$ -dependent non-resonant phases to be  $\delta_C(\xi) = \delta_U(\xi) = 0$ . Under these circumstances, the PDF of Eq. (12) depends on four cosine terms that are measured in the experiment:

$$\begin{aligned} c_{00}^{\pm} &\equiv \cos(\delta_{\mathcal{U}0} \pm \gamma) \\ c_{K^*0}^{\pm} &\equiv \cos(\delta_{\mathcal{U}0} - \delta_{K^*} - \delta_{K^*}(\xi) \pm \gamma), \end{aligned} \quad (14)$$

where  $\delta_{K^*}(\xi)$  is the  $\xi$ -dependent  $K^*$  Breit-Wigner phase of Eq. (10). The cosines  $c_{00}^{\pm}$  ( $c_{K^*0}^{\pm}$ ) arise from interference between the non-resonant (resonant)  $\bar{b} \rightarrow \bar{c}u\bar{s}$  amplitude and the non-resonant  $\bar{b} \rightarrow \bar{u}c\bar{s}$  amplitude.

The phases  $\delta_{\mathcal{U}0}$ ,  $\delta_{K^*}$ , and  $\gamma$  are all *a-priori* unknown. However, it is important to note that  $\delta_{K^*}$  is fully determined from the interference between the resonant and non-resonant contributions to the relatively high statistics decay mode  $B^+ \rightarrow \bar{D}^0 K^+ \pi^0$  as a function of the Dalitz plot variables. Therefore,  $\delta_{K^*}$  is obtained with no ambiguities, and with an error much smaller than those of  $\delta_{\mathcal{U}0}$  or  $\gamma^*$ . Consequently, the only relevant symmetry operations are

$$\begin{aligned} S_{\text{ex}} &: \gamma \rightarrow \delta_{\mathcal{U}0} & , \delta_{\mathcal{U}0} \rightarrow \gamma \\ S_{\text{sign}} &: \gamma \rightarrow -\gamma & , \delta_{\mathcal{U}0} \rightarrow -\delta_{\mathcal{U}0} \\ S_{\pi} &: \gamma \rightarrow \gamma + \pi & , \delta_{\mathcal{U}0} \rightarrow \delta_{\mathcal{U}0} + \pi \\ S_{\text{ex}}^{K^*+} &: \gamma \rightarrow \delta_{\mathcal{U}0} - \delta_{K^*} & , \delta_{\mathcal{U}0} \rightarrow \gamma + \delta_{K^*} \\ S_{\text{ex}}^{K^*-} &: \gamma \rightarrow -\delta_{\mathcal{U}0} + \delta_{K^*} & , \delta_{\mathcal{U}0} \rightarrow -\gamma + \delta_{K^*}. \end{aligned} \quad (15)$$

As discussed above, only  $S_{\pi}$  is a symmetry of all four cosines of Eq. (14), and is therefore fully unresolved. The transformation properties of the cosines under any combination of the remaining four operations that can lead to an ambiguity are shown in Table I.

TABLE I. Invariance of each of the cosines of Eq. (14) under combinations of the symmetry operations of Eq. (15), excluding  $S_{\pi}$ . Full invariance (approximate invariance) is indicated by a  $\checkmark$  ( $\checkmark$ ).

Operation	$c_{K^*0}^+$	$c_{K^*0}^-$	$c_{00}^+$	$c_{00}^-$
Non-resonant regime				
$S_{\text{ex}}$	$\checkmark$		$\checkmark$	$\checkmark$
$S_{\text{sign}}$			$\checkmark$	$\checkmark$
$S_{\text{ex}}S_{\text{sign}}$		$\checkmark$	$\checkmark$	$\checkmark$
Resonant regime				
$S_{\text{ex}}^{K^*+}$	$\checkmark$	$\checkmark$	$\checkmark$	$\checkmark$
$S_{\text{ex}}^{K^*-}$	$\checkmark$	$\checkmark$		$\checkmark$
$S_{\text{ex}}^{K^*+}S_{\text{ex}}^{K^*-}$	$\checkmark$	$\checkmark$	$\checkmark$	

\*Even when one of the  $\bar{b} \rightarrow \bar{c}u\bar{s}$  amplitudes is small enough that the determination of  $\delta_{K^*}$  becomes difficult, one effectively has  $\delta_{\mathcal{U}0} \rightarrow \delta_{\mathcal{U}0} - \delta_{K^*}$ ,  $\delta_{K^*} \rightarrow 0$ , and the determination of  $\delta_{K^*}$  is again not a problem.

While none of the operations leaves all four cosines invariant, it is important to note cases where  $c_{K^*0}^\pm$  are *approximately* invariant under  $S_{\text{ex}}^{K^*+}$ ,  $S_{\text{ex}}^{K^*-}$ , or their product. We define approximate invariance under the operation  $S$  to be

$$S_{\text{app}} c_{K^*0}^\pm(\delta_{K^*}(\xi)) = c_{K^*0}^\pm(-\delta_{K^*}(\xi)). \quad (16)$$

Approximate invariance arises due to the fact that far from the peak of the  $K^*$  resonance,  $\delta_{K^*}(\xi)$  changes slowly as a function of the  $K\pi$  invariant mass, and takes values around 0 and  $\pi$ . Therefore, for events in the tails of the Breit-Wigner,  $\delta_{K^*}(\xi)$  is almost invariant under any  $S_{\text{app}}$  satisfying Eq. (16). One can see that approximate invariance of one of the cosines  $c_{K^*0}^\pm$  implies minimal change in the  $\chi^2$  of Eq. (13), which may result in a resolved yet clearly observable ambiguity. Since both  $c_{K^*0}^\pm$  terms are only approximately invariant under the product  $S_{\text{ex}}^{K^*+}S_{\text{ex}}^{K^*-}$ , this ambiguity is more strongly resolved than either  $S_{\text{ex}}^{K^*+}$  or  $S_{\text{ex}}^{K^*-}$ .

Observing that no single operation in the Table I is a good symmetry of all cosines, one identifies two different regimes: In the non-resonant regime, interference with the non-resonant  $\bar{b} \rightarrow \bar{c}u\bar{s}$  is dominant, and only  $S_{\text{ex}}$  and  $S_{\text{sign}}$  may lead to ambiguities. In the resonant regime, the  $K^*$  amplitude strongly dominates the  $\bar{b} \rightarrow \bar{c}u\bar{s}$  decay, and  $S_{\text{ex}}^{K^*+}$  and  $S_{\text{ex}}^{K^*-}$  become the important ambiguities. In the transition between these regimes, the operations of Table I do not lead to clear ambiguities, as we have verified by simulation (See sec. V). Thus, while naively one may expect a 2<sup>5</sup>-fold ambiguity, in practice the observable ambiguity is no larger than eight-fold, with only the two-fold  $S_\pi$  being fully unresolved, in the likely case of non-negligible resonant contribution. This is demonstrated in Fig. 8. Furthermore, although one may write down more products of the operations  $S_{\text{ex}}$ ,  $S_{\text{sign}}$ ,  $S_{\text{ex}}^{K^*+}$ , and  $S_{\text{ex}}^{K^*-}$ , only the products listed in Table I result in full or partial invariance of both cosines which dominate the same regime. The additional products do not result in any noticeable ambiguities.

## V. MEASUREMENT SENSITIVITY AND SIMULATION STUDIES

To study the feasibility of the analysis using Eq. (13) and verify the predictions of Sec. IV, we conducted a simulation of the decays  $B^\pm \rightarrow D^0 K^\pm \pi^0$ ,  $B^\pm \rightarrow \bar{D}^0 K^\pm \pi^0$ , and  $B^\pm \rightarrow D_{1,2} K^\pm \pi^0$ . Events were generated according to the PDF of Eq. (12), with the base parameter values given in Table II. In this table and throughout the rest of the paper, we use a tilde to denote the “true” parameter values used to generate events, while the corresponding plain symbols represent the “trial” parameters used to calculate the experimental  $\chi^2$ .

The only non-vanishing amplitudes in the simulation were the non-resonant amplitudes in the  $\bar{b} \rightarrow \bar{c}u\bar{s}$  and  $\bar{b} \rightarrow \bar{u}c\bar{s}$  decays, and the  $K^*$  resonant  $\bar{b} \rightarrow \bar{c}u\bar{s}$  amplitude. For simplicity, additional resonances were not included in this demonstration. However, broad resonances that are observed in the data should be included in the actual data analysis.

The simulations were conducted with a benchmark integrated luminosity of 400  $\text{fb}^{-1}$ , which each of the asymmetric B-factories plan to collect by about 2005. The final state reconstruction efficiencies were calculated based on the capabilities of current  $\Upsilon(4\text{S})$  detectors. We assumed an efficiency of 70% for reconstructing the  $K^\pm$ , including track quality and particle identification requirements, and 60% for reconstructing the  $\pi^0$ . The product of reconstruction efficiencies and branching fractions of the  $D^0$ , summed over the final states

TABLE II. Parameters used to generate events in the simulation. The value of  $\tilde{A}_{CK^*}$  is chosen so as to roughly agree with the measurement of the corresponding branching fraction [22], taking into account the  $K^{*+} \rightarrow K^+ \pi^0$  branching fraction.

Parameter	Value	Parameter	Value
$\tilde{\gamma}$	1.20	$\tilde{A}_{U0}/\tilde{A}_{C0}$	0.4
$\tilde{\delta}_C(\xi) = \tilde{\delta}_U(\xi)$	0	$\tilde{A}_{CK^*}/\tilde{A}_{C0}$	1.0
$\tilde{\delta}_{K^*}$	1.8	$\tilde{A}_{CK^*}$	$\sim \sqrt{2 \times 10^{-4} \Gamma_B}$
$\tilde{\delta}_{U0}$	0.4		

TABLE III. The numbers of events obtained by averaging 100 simulations using the parameters of Table II and the reconstruction efficiencies listed in the text.

Mode	Signal events per $400\text{fb}^{-1}$
$B^+ \rightarrow \overline{D^0} K^+ \pi^0 = B^- \rightarrow D^0 K^- \pi^0$	2610
$B^+ \rightarrow D^0 K^+ \pi^0 = B^- \rightarrow \overline{D^0} K^- \pi^0$	205
$B^+ \rightarrow D_{1,2} K^+ \pi^0$	186
$B^- \rightarrow D_{1,2} K^- \pi^0$	234

$K^- \pi^+$ ,  $K^- \pi^+ \pi^0$ , and  $K^- \pi^+ \pi^- \pi^+$ , is taken to yield an effective efficiency of 6%. Using the CP-eigenstate final states  $K^+ K^-$ ,  $\pi^+ \pi^-$ ,  $K_S \pi^0$ , and  $K_S \rho^0$ , the effective efficiency for the sum of the  $D_1$  and  $D_2$  final states is 0.8%. All efficiencies are further reduced by a factor of 1.7, in order to approximate the effect of background. The numbers of signal events obtained in each of the final states with the above efficiencies and the parameters of Table II are listed in Table III.

In Figs. 6 through 8, we show the dependence of  $\chi^2$  on the values of  $\gamma$  and  $\delta_{U0}$ . The smallest value of  $\chi^2$  is shown as zero. At each point in these figures,  $\chi^2$  is calculated with the generated values of the amplitude ratios  $A_{U0}/A_{C0} = \tilde{A}_{U0}/\tilde{A}_{C0}$  and  $A_{CK^*}/A_{C0} = \tilde{A}_{CK^*}/\tilde{A}_{C0}$ . We note that when these amplitude ratios are determined by a fit simultaneously with the phases, the correlations between the amplitudes and the phases are generally found to be less than 20%. Therefore, the results obtained with the amplitudes fixed to their true values are sufficiently realistic for the purpose of this demonstration.

For each of these figures, we also show the one-dimensional minimum projection  $\chi^2(\gamma) = \min\{\chi^2(\gamma, \delta_{U0})\}$ , showing the smallest value of  $\chi^2$  for each value of  $\gamma$ .

Fig. 6 is a simulation obtained with the parameters of Table II, but with  $A_{CK^*} = 0$ . With no resonant contribution, the eight-fold ambiguity of the perfect non-resonant regime is clearly visible. This would be the typical case for two-body final states.

Fig. 7 is obtained with the parameters of Table II, but with  $A_{C0} = 0$ . With no non-resonant  $\bar{b} \rightarrow \bar{c} u \bar{s}$  contribution, the eight-fold ambiguity of the perfect resonant regime is seen. The ambiguities corresponding to approximate invariance are clearly resolved, with

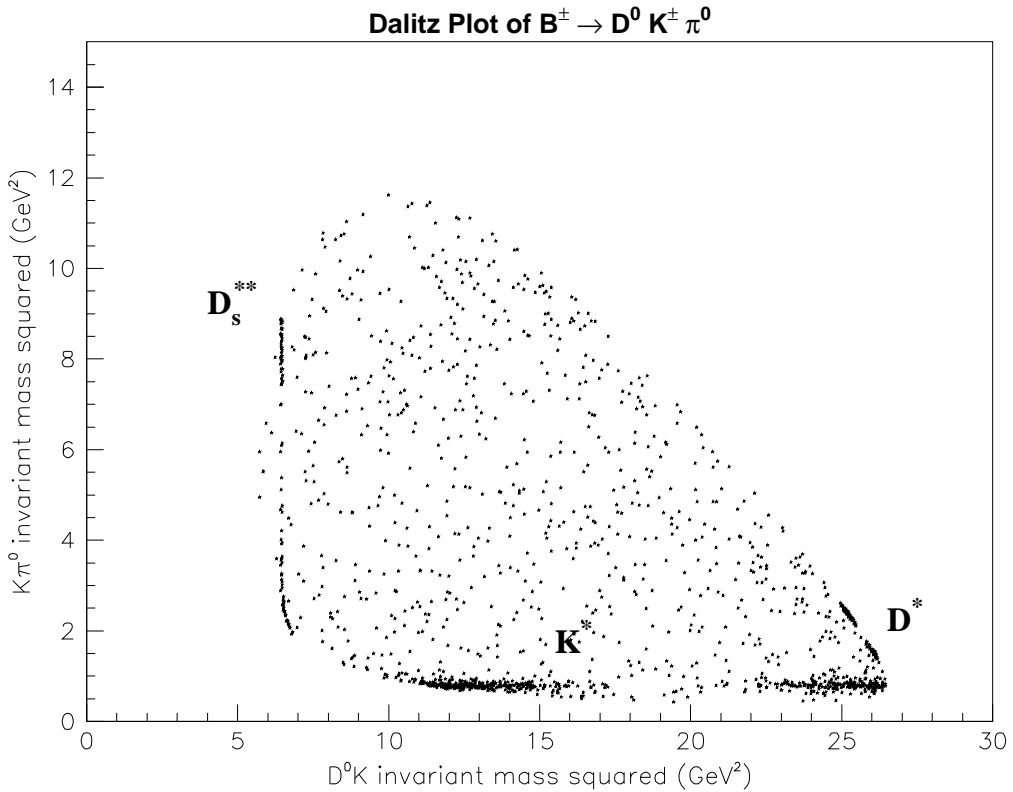


FIG. 5. Dalitz plots obtained from a simulation of  $B^+$  and  $B^-$  decays into all final state,  $D^0 K^\pm \pi^0$ ,  $\overline{D^0} K^\pm \pi^0$ , and  $D_{1,2} K^\pm \pi^0$ . with the parameters of Table II. Along with non-resonant contributions, the resonances  $K^{*0}$ ,  $D^{*0}$ , and  $D_s^{**}$  are shown.

the doubly-approximate  $S_{\text{ex}}^{K^*+} S_{\text{ex}}^{K^*-}$  ambiguity resolved more strongly.

Fig. 8 is obtained with the parameters of Table II and shows how efficient the method described in this paper could be for extracting the angle  $\gamma$ . With equal resonant and non-resonant  $\bar{b} \rightarrow \bar{c}u\bar{s}$  amplitudes, only the non-resonant regime ambiguities are observed, due to the relative suppression of the resonant interference terms discussed in Sec. IV. Nonetheless, the  $c_{K^*0}^\pm$  terms are significant enough to resolve all but the  $S_\pi$  ambiguity.  $S_{\text{sign}}$  is more strongly resolved, since it leaves neither of the  $c_{K^*0}^\pm$  terms invariant.

Also shown in Fig. 8 (dashed line) is the minimum projection of  $\chi^2(\gamma)$  of the average experiment. This plot is obtained by averaging over  $\chi^2(\gamma)$  of 50 simulated experiments, each generated with the parameters of Table II, but with different initial random numbers. The three standard deviation region of  $\gamma$  allowed by the average experiment is indicated. This region spans the range  $[-0.06, 1.65]$ , giving an idea of the sensitivity that may be obtained with these parameter values.

In Figs. 9 through 12 we present  $\sigma_\gamma$ , the statistical error in the measurement of  $\gamma$ , obtained by fitting simulated event samples using the MINUIT package [23], as a function of one of the parameters of Table II. All the other parameters were kept at the values listed in Table II.

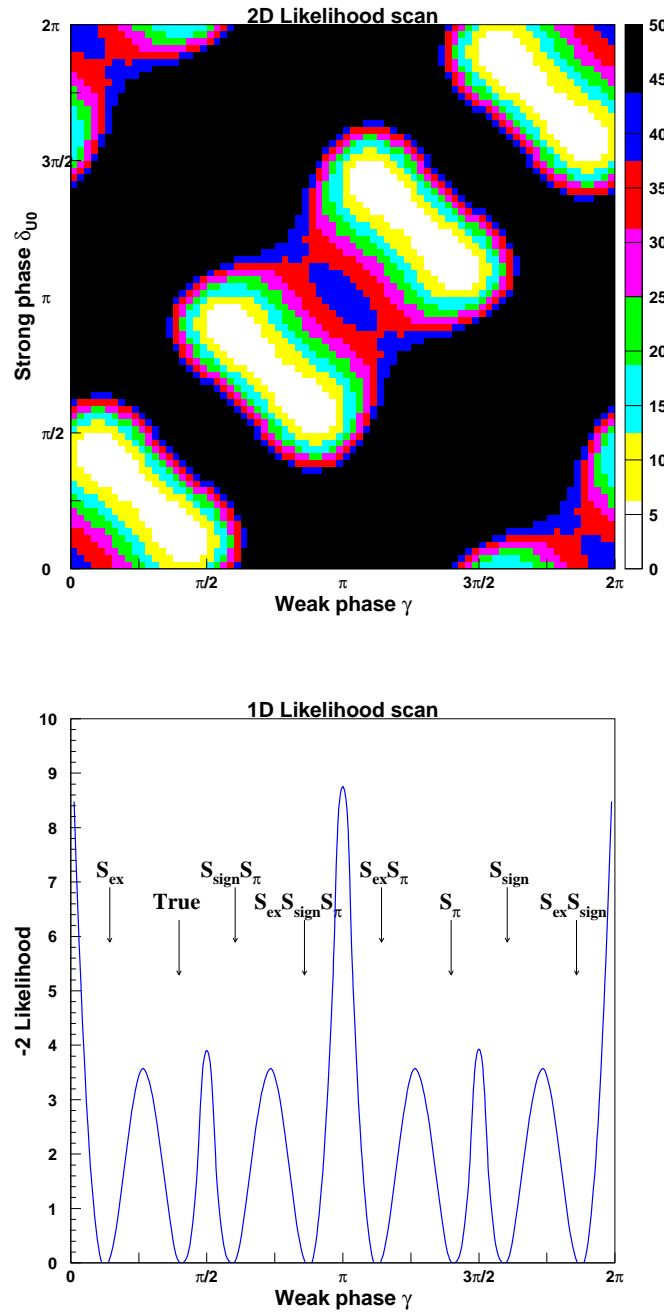


FIG. 6. **Top:**  $\chi^2$  as a function of  $\gamma$  and  $\delta_{U0}$ , with the parameters of Table II and no resonant contribution ( $\tilde{A}_{CK^*} = 0$ ). **Bottom:** Minimum projection of  $\chi^2$  onto  $\gamma$ .

Each point in these plots is obtained by repeating the simulation 250 times, to minimize sample-to-sample statistical fluctuations. In all cases, all the parameters of Table II were determined by the fit. The arrows in these figures indicate the point corresponding to the parameters of Table II. The total number of signal events in all final states combined is the

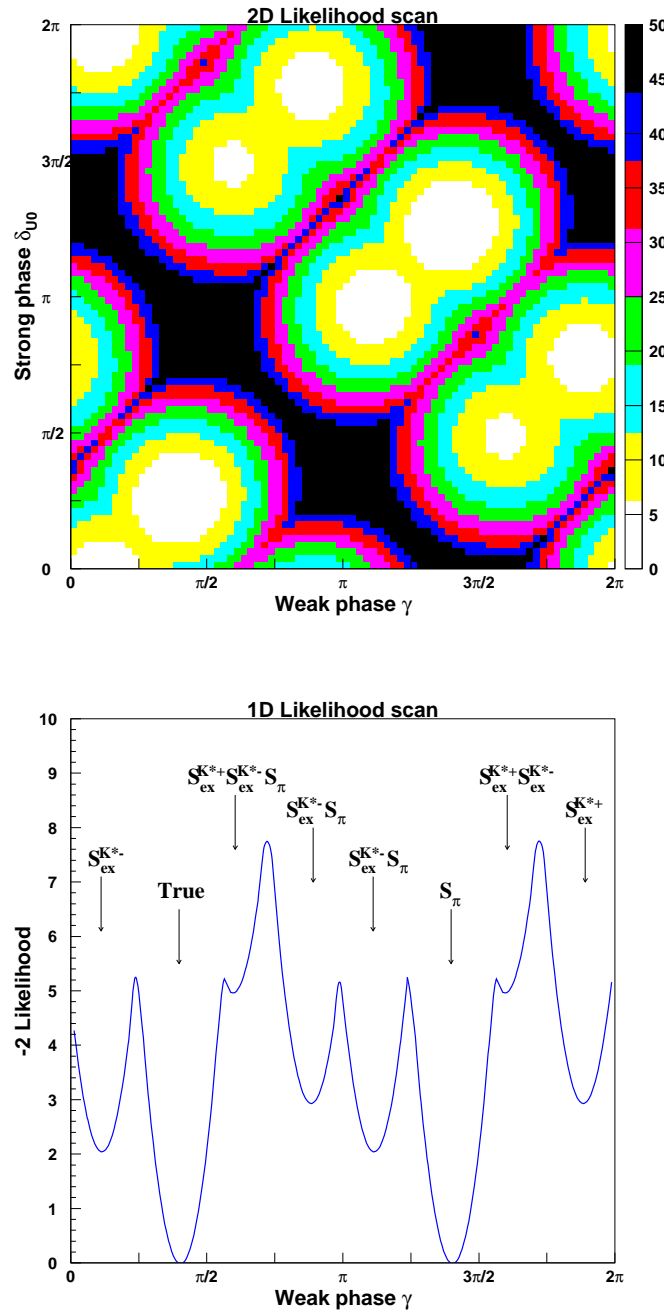


FIG. 7. **Top:**  $\chi^2$  as a function of  $\gamma$  and  $\delta_{\mathcal{U}0}$ , with no non-resonant  $\bar{b} \rightarrow \bar{c}u\bar{s}$  contribution ( $\tilde{A}_{C0} = 0$ ). The value  $\delta_{K^*} = 1.2$  is used to ensure that ambiguities do not overlap. All other parameters are those of Table II. **Bottom:** Minimum projection of  $\chi^2$  onto  $\gamma$ .

same for each of the data points. The error bars describe the statistical error at each point, which is determined by the number of experiments simulated.

One observes that  $\sigma_\gamma$  does not depend strongly on  $\tilde{\delta}_{K^*}$ , and has a mild dependence on

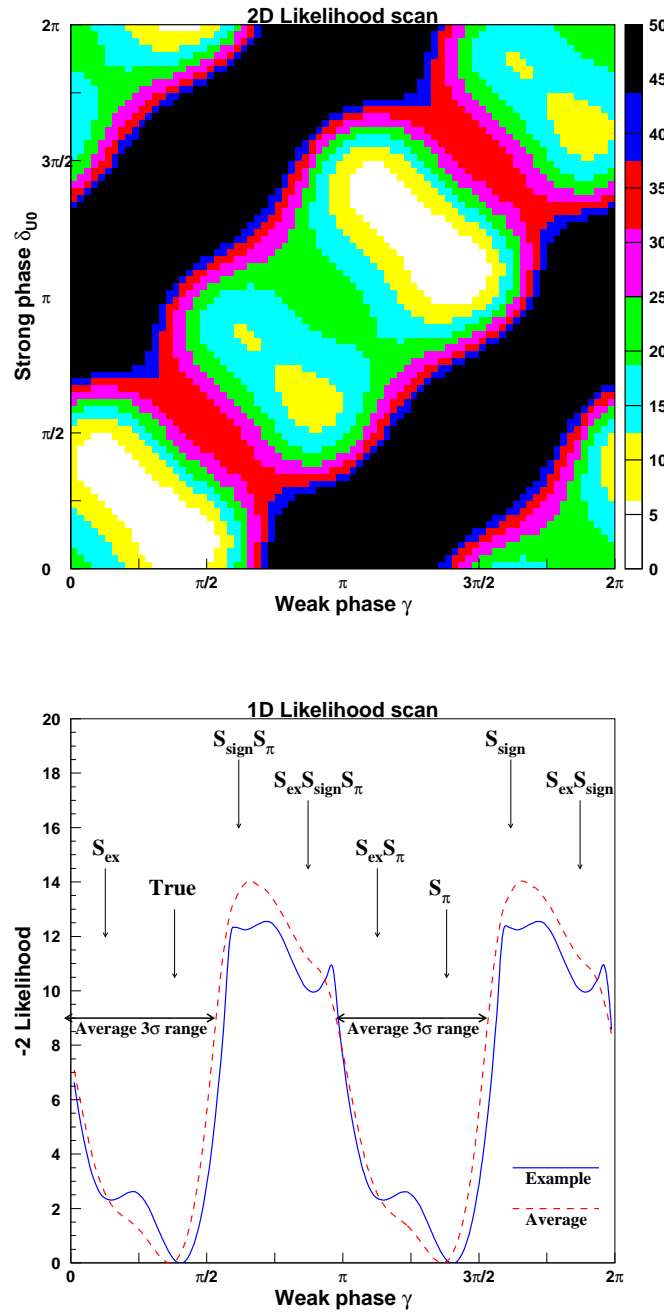


FIG. 8. **Top:**  $\chi^2$  as a function of  $\gamma$  and  $\delta_{U0}$ , with the parameters of Table II. **Bottom:** The solid line shows the minimum projection of  $\chi^2$  onto  $\gamma$  for the example experiment. The dashed line represents the average of 50 simulated experiments. The three standard deviation allowed range of  $\gamma$  obtained from the average is indicated by arrows.

$\tilde{\delta}_{U0}$ . As expected, strong dependence on  $\tilde{A}_{U0}/\tilde{A}_{C0}$  is seen in Fig. 12. However, it should be noted that  $\sigma_\gamma$  changes very little for all values of  $\tilde{A}_{U0}/\tilde{A}_{C0}$  above about 0.4, given that

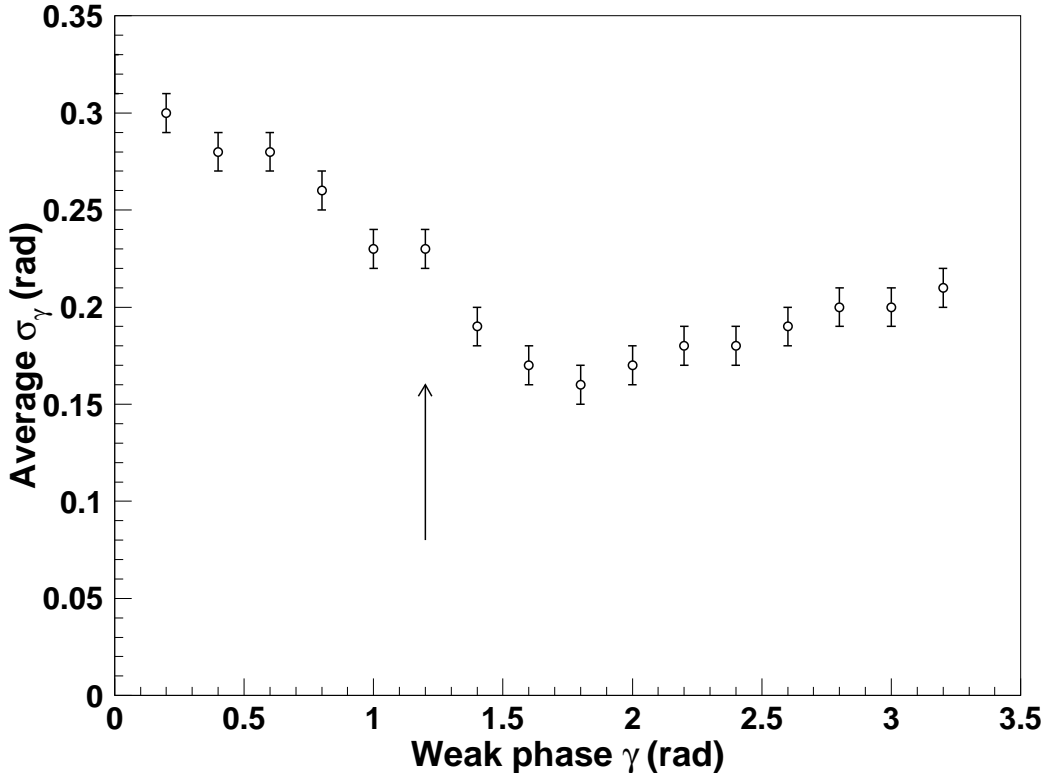


FIG. 9. The error in  $\gamma$ ,  $\sigma_\gamma$ , as a function of  $\tilde{\gamma}$ .

the total number of signal events in all modes was kept constant in our simulation. This suggests that the likelihood for a significantly sensitive measurement is high over a broad range of parameters. With the parameters of Table II, we find  $\sigma_\gamma \approx 0.23 = 13^\circ$  with an integrated luminosity of  $400 \text{ fb}^{-1}$ .

## VI. CONCLUSIONS

We have shown how  $\gamma$  may be measured in the color-allowed decays  $B \rightarrow D^{(*)}K^{(*)}\pi(\rho)$ , focusing on the simplest mode  $B^\pm \rightarrow D^0K^\pm\pi^0$ . The absence of color suppression in the  $\bar{b} \rightarrow \bar{u}c\bar{s}$  amplitudes is expected to result in relatively large rates and significant CP violation effects, and hence favorable experimental sensitivities. Although the Dalitz plot analysis required for this purpose constitutes some experimental complication, it should not pose a major difficulty, while being very effective at reducing the eight-fold ambiguities that constitute a serious limitation with other methods for measuring  $\gamma$ . Only the two-fold  $S_\pi$  ambiguity cannot be resolved solely by our method, requiring additional constraints from other measurements of the unitarity triangle. As a result of these advantages, this method is likely to lead to relatively favorable errors and provide a significant measurement of  $\gamma$ ,

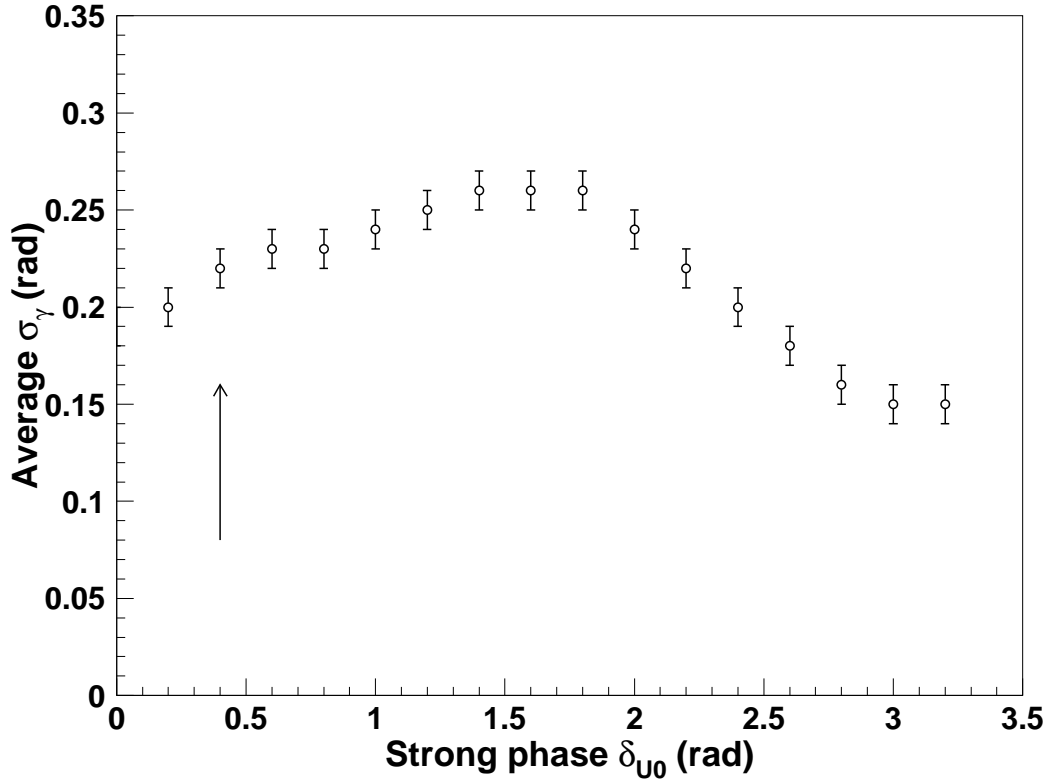


FIG. 10. The error in  $\gamma$ ,  $\sigma_\gamma$ , as a function of  $\tilde{\delta}_{U0}$ .

even with the current generation of B factory experiments.

## VII. ACKNOWLEDGMENTS

The authors thank Francois Le Diberder for his fruitful ideas and help with simulation. This work was supported by the Danish Research Agency, the CEA and CNRS-IN2P3 (France), and by the U.S. Department of Energy under contracts DE-AC03-76SF00515 and DE-FG03-93ER40788.

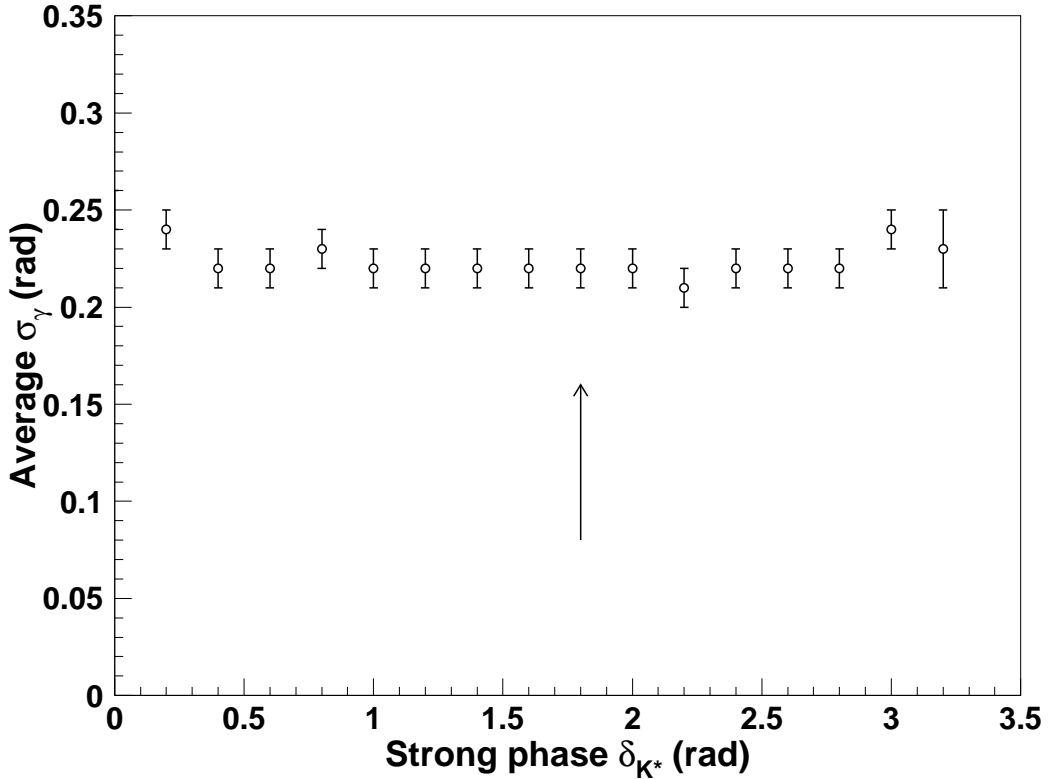


FIG. 11. The error in  $\gamma$ ,  $\sigma_\gamma$ , as a function of  $\tilde{\delta}_{K^*}$ .

## REFERENCES

- [1] N. Cabibbo, *Phys. Rev. Lett.* **10**, 531 (1963); M. Kobayashi and K. Maskawa, *Prog. Theor. Phys.* **49** (1973), 652.
- [2] BaBar Collaboration (B. Aubert *et al.*), *Phys. Rev. Lett.* **86** (2001), 2515.
- [3] Belle Collaboration (B. Abe *et al.*), *Phys. Rev. Lett.* **87** (2001), 091802.
- [4] R. Aleksan, I. Dunietz and B. Kayser, *Z. Phys. C* **54** (1992), 653.
- [5] A. Soffer, *Phys. Rev.* **D60** (1999), 054032; A. Soffer, Proceedings, Snowmass 2001 Workshop on the Future of High Energy Physics, 2001.
- [6] M. Gronau and D. Wyler, *Phys. Lett.* **B265** (1991), 172.
- [7] I. Dunietz, *Phys. Lett.* **B270** (1991), 75.
- [8] D. Atwood, G. Eilam, M. Gronau, and A. Soni, *Phys. Lett.* **B341** (1995), 372.
- [9] J.H. Jang and P. Ko, *Phys. Rev.* **D58** (1998), 111302.
- [10] M. Gronau and J.L. Rosner, *Phys. Lett.* **B439** (1998), 171.
- [11] D. Atwood, I. Dunietz, and A. Soni, *Phys. Rev. Lett.* **78** (1997), 3257.
- [12] J.P. Silva and A. Soffer, *Phys. Rev.* **D61** (2000), 112001.
- [13] A. Soffer, hep-ex/9801018 (1998).
- [14] CLEO Collaboration (B. Barish *et al.*), CLEO CONF 97-01, EPS 339.

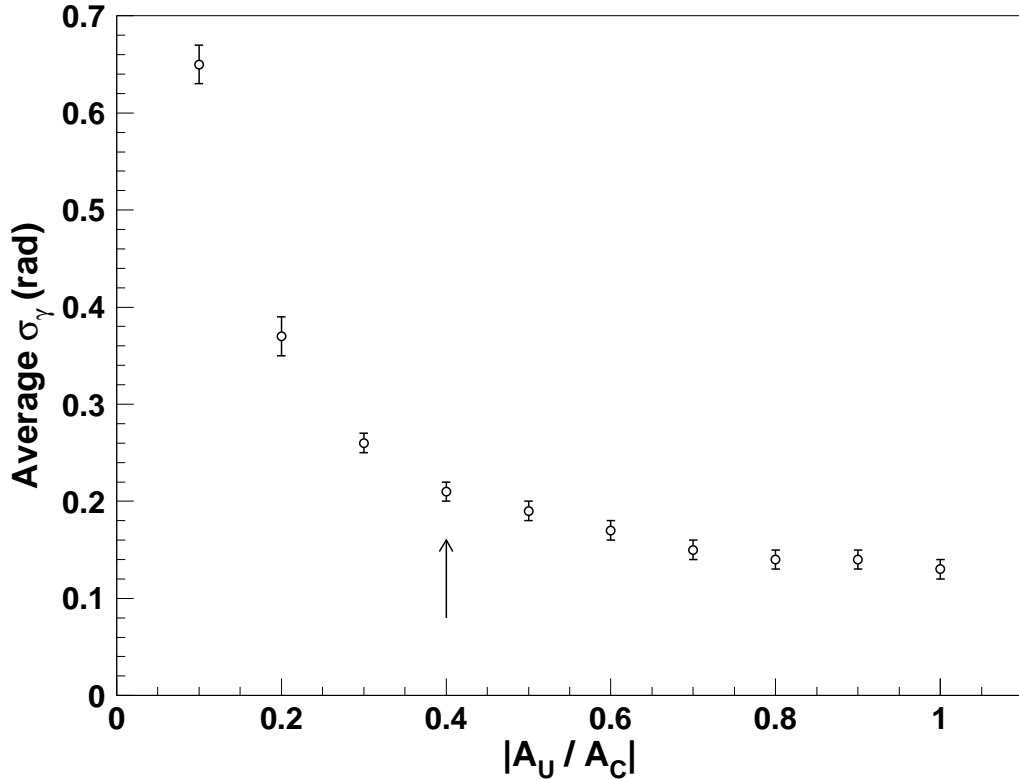


FIG. 12. The error in  $\gamma$ ,  $\sigma_\gamma$ , as a function of  $\tilde{A}_{U0}/\tilde{A}_{C0}$ .

- [15] Belle Collaboration (B. Abe *et al.*), hep-ex/0109021 (2001).
- [16] CLEO Collaboration (T.E. Coan *et al.*), hep-ex/0110055 (2001).
- [17] R. Aleksan *et al.*, in preparation.
- [18] L. Wolfenstein, Phys. Rev. Lett. **51** (1983) 1945.
- [19] R. Aleksan, B. Kayser and D. London, Phys. Rev. Lett. **73**, (1994) 18.
- [20] See, for example, J.C. Anjos *et. al.*, Phys. Rev. **D48**, 56 (1992).
- [21] Belle Collaboration (B. Abe *et al.*), Preprint BELLE-CONF-0235 (2002).
- [22] The CLEO Collaboration, Phys. Rev. Lett. 88, 101803 (2002).
- [23] F. James, M. Roos, Comput. Phys. Commun. **10** 343 (1975).